Sustainable Carbon Materials

https://doi.org/10.48130/scm-0026-0023

Original Research

Open Access

Reusable magnetic SERS platform functionalized with covalent organic polymers for trace-level and machine-learning-assisted uranyl detection

Wentao Zhang[1], Jing Ma[1], Yiyan Zhang[1], Suhua Wang[2], Muhammad Wakeel[3] and Zhenli Sun[1*]

Received: 16 January 2026

Revised: 17 April 2026

Accepted: 25 May 2026

Published online: 27 July 2026

Abstract

The sustainable development of nuclear energy relies on efficient and reliable monitoring of uranium species in environmental systems. However, trace-level uranyl ions (UO_2^{2+}) remain challenging to detect due to their low concentration and complex chemical environment. Herein, a reusable magnetic surface-enhanced Raman scattering (SERS) substrate, FA@tPF, is developed. It is based on Fe_3O_4@SiO_2@Au microspheres functionalized with a polyarylene ether-based covalent organic polymer (tPF). The substrate exhibits high chemical stability and strong affinity toward uranyl ions. Comprehensive characterization via SEM, FT-IR, and XPS confirmed the successful construction of the FA@tPF nanocomposite with optimized surface morphology. The substrate enabled sensitive detection of UO_2^{2+} with a detection limit of 1×10^{-7} mol·L^{-1} under 20 min enrichment, and its magnetic solid-phase microextraction capability allows for further improvement in detection limits with extended collection time, along with strong selectivity and robust reusability through Na_2CO_3-assisted desorption. Spectral classification using principal component analysis and a convolutional neural network model achieved 100% accuracy, while gradient-weighted class activation map-based interpretation confirmed that uranyl-specific bands (~850 cm^{-1}) dominantly contributed to model decisions. These results demonstrate that FA@tPF serves as a chemically selective and reusable SERS platform integrated with interpretable machine learning, offering an intelligent and sustainable solution for uranyl detection in complex environments and ensuring nuclear environmental safety.

Keywords: Uranyl detection, SERS, Covalent organic polymers, Reusable, Machine learning

Highlights

- A reusable magnetic SERS platform was developed by integrating plasmonic nanostructures with a carbon-rich covalent organic polymer.
- The polyarylether-based tPF forms a chemically robust, carbon-dominated functional framework with strong affinity toward UO_2^{2+}.
- Hotspot-localized enrichment enables sensitive uranyl detection down to 1×10^{-7} mol·L^{-1} with excellent selectivity and recyclability.
- Interpretable machine learning allows accurate spectral identification and reveals uranyl-specific Raman fingerprints.

* Correspondence: Zhenli Sun (sunliva@ncepu.edu.cn)

Full list of author information is available at the end of the article.

https://doi.org/10.48130/scm-0026-0023

Graphical abstract

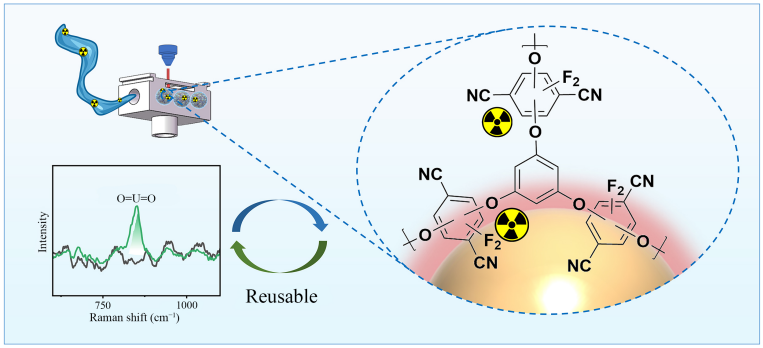

Introduction

The sustainable development of nuclear energy critically depends on the safe management of uranium, whose environmental release poses serious threats to both ecosystems and human health. Uranium exists as a dual-risk element with combined radiotoxicity and chemical toxicity, particularly in aquatic systems where its high mobility promotes migration and bioaccumulation[1–3]. Epidemiological and experimental studies have associated uranium exposure with neurological, respiratory, and cardiovascular disorders, underscoring its potential health hazards[4]. Given the rising demand for clean and safe nuclear technologies, it is imperative to develop rapid, sensitive, and selective analytical tools for real-time monitoring of uranium species, particularly uranyl ions (UO_2^{2+}) in complex environmental matrices. Such capabilities are essential not only for environmental surveillance but also for ensuring the sustainability and safety of nuclear energy systems[5,6].

Current techniques, such as inductively coupled plasma mass spectrometry, voltammetry, atomic absorption spectroscopy, atomic emission spectroscopy, and X-ray fluorescence spectroscopy, provide high sensitivity and accuracy for uranyl detection[7–10]. However, these methods typically require expensive equipment, complex sample preparation, and skilled operations, limiting their application in real-time on-site monitoring[11]. In contrast, surface-enhanced Raman scattering (SERS) offers a promising alternative with ultrafast analysis, high sensitivity, and the ability to provide structural information through vibrational fingerprints[12–16]. SERS enables non-destructive, on-site detection, making it ideal for monitoring uranyl ions in contaminated environments.

The effectiveness of SERS critically hinges on substrate properties, which must enhance Raman signals while maintaining high selectivity and stability in complex matrices. Recent studies have explored the use of porous nanomaterials, particularly metal-organic frameworks (MOFs) and covalent organic frameworks (COFs), as potential SERS substrates for uranyl ion detection[17–20]. Additionally, covalent organic polymers (COPs) have gained significant attention due to their robust covalent frameworks and versatile functionalization[21]. COPs possess unique physicochemical properties that make them ideal for the selective adsorption and detection of target analytes. For instance, Xiao et al.[22] developed a COP (HT-COP-AO) that demonstrated strong uranium coordination, enabling it to function both as a fluorescent probe and an adsorbent. Similarly, Leng et al.[23] synthesized a polyarylether-based COP (tPF-AO) through a simple condensation reaction and surface modification, which was specifically designed for selective uranyl ion capture and detection. The polyarylether structure imparts high stability under acidic, alkaline, and seawater conditions. The material exhibits excellent selectivity, recyclability, and an adsorption capacity of 578.9 ± 15.2 mg·g^{-1}, making it promising for SERS-based detection of trace uranyl ions. Therefore, COPs show considerable potential for SERS-based trace uranyl ion detection.

Building upon the advantages of COPs, this study develops a novel reusable magnetic SERS substrate, FA@tPF, specifically designed for the sensitive detection of uranyl ions. The tPF layer effectively adsorbs uranyl ions and directs them into hot spots between AuNPs, thereby enhancing SERS signals. The magnetic properties of the substrate enable uniform adsorption, as well as rapid enrichment and separation of SERS-active substances. The developed technique achieves highly sensitive detection of uranyl ions through magnetic separation and selective adsorption. To further enhance detection robustness and interpretability, machine learning algorithms including principal component analysis (PCA), convolutional neural network (CNN), and gradient-weighted class activation map (Grad-CAM) were integrated to classify spectral features and reveal chemically meaningful Raman shifts. This integrated strategy offers a chemically selective, reusable, and intelligent SERS platform for real-time uranyl ion monitoring.

Materials and methods

Materials

All reagents were analytical grade and used as received. The following chemicals were obtained from Sinopharm: chloroauric acid tetrahydrate ($HAuCl_4{\cdot}4H_2O$, 47.8% Au basis), crystal violet (CV), ammonium uranyl nitrate hexahydrate ($UO_2[NO_3]_2{\cdot}6H_2O$), 4-mercaptopyridine (4-MPY), ethylene glycol (EG), and concentrated HNO_3. Poly(diallyldimethylammonium chloride) (PDDA) and TEOS were acquired from Sigma-Aldrich. The following reagents were acquired from Aladdin: anhydrous sodium citrate (Na_3Ct), N,N-dimethylformamide (DMF), and K_2CO_3. Tetrahydrofuran (THF) was purchased from MACKLIN Reagents. In addition, phloroglucinol (tP) and 2,3,5,6-tetrafluoroterephthalonitrile (TFTPN) were purchased from the Tansoole platform. Tap water used in the experiments was obtained from the laboratory.

Synthesis of FA@tPF

Magnetic FA nanoparticles (30 mg) were synthesized according to a published protocol[24]. For the synthesis of the tPF layer on the FA surface, a modified method based on the literature was employed[23].

To a THF/DMF solution (16:1, 10 mL) were added tP (0.1 mmol), TFTPN (0.15 mmol), and K_2CO_3 (2.2 mmol) sequentially. After sonication for 10 min, 1.5 mL of FA was added, and the solution was purged with N_2 gas for 5 min. The mixture was reacted at 85 °C with continuous stirring (500 rpm) over 48 h. The resulting solid product was washed thoroughly with DMF, THF, anhydrous ethanol, and DI water to obtain the FA@tPF substrate.

Characterization

In Raman spectroscopic analysis, 20 μL of the synthesized FA@tPF substrate was mixed with 4.5 mL of a standard uranium solution and shaken for 20 min. The magnetic substrate was then collected using a magnet, and the supernatant was removed. The enriched magnetic material was deposited onto a silicon wafer, and a cylindrical magnet was placed underneath to help concentrate the sample and form a uniformly thin film. For the flow-through cell experiment, the water sample was continuously introduced into the flow-through cell at a constant flow rate of 2.5 mL·min^{-1}, and the SERS signal was recorded at different flow times (1–20 min) to evaluate the dynamic enrichment process. The sample continuously interacted with the FA@tPF substrate immobilized on the silicon wafer under an external magnetic field, enabling efficient analyte enrichment and real-time detection. SERS measurements were performed on a PERS-RZ1702B portable Raman spectrometer with the following parameters: 785 nm laser excitation with 4 cm^{-1} spectral resolution, 250 mW actual laser power (50% of 500 mW total power), and 4 s acquisition time. The laser spot diameter was approximately 0.3 mm. The material morphology was analyzed using Hitachi JEM-2800 TEM and S-4800 FE-SEM systems. XPS analysis (Thermo ESCALAB 250xi) characterized FA@tPF both prior to and following uranyl ion adsorption.

FDTD simulation details

The FDTD simulation was based on our previously reported FA model[24]. Au nanoparticles were constructed according to TEM/SEM observations, with an average particle size of ~20 nm and an interparticle gap of ~5 nm, and were approximated as densely assembled satellite structures on the Fe_3O_4@SiO_2 surface. A 785 nm plane wave was used to match experimental conditions. The electromagnetic field distribution was calculated by solving Maxwell's equations in three dimensions with a mesh size of 1 nm and a simulation time of 1,000 fs.

Machine learning-based spectral analysis

Uranyl SERS spectra collected from FA, FA@ZIF-8, and FA@tPF substrates at a fixed concentration of 1×10^{-5} mol·L^{-1} were used for machine learning analysis. Spectral data were truncated to the 600–1,000 cm^{-1} region and standardized using z-score normalization via the StandardScaler method. PCA was performed to reduce data dimensionality and visualize the separability of spectral clusters. Spectra were analyzed using a CNN model. The CNN framework is based on a two-layer convolutional layer design, each equipped with batch normalization and ReLU activation functions, as well as subsequent Dropout and MaxPooling to enhance the generalization of the model. The dataset used for model training and validation contained two categories. SERS spectra collected from FA@tPF substrates adsorbed with uranyl ions at concentrations of 1×10^{-4}, 1×10^{-5}, 1×10^{-6}, and 1×10^{-7} mol·L^{-1} were defined as positive, while SERS spectra of FA@tPF substrates without uranyl adsorption were defined as negative. The numbers of both categories were harmonized to the same level using data enhancement techniques to avoid classification convergence bias. To further explain the decision basis of the model, the Grad-CAM algorithm was embedded into the CNN model so that the model could generate heat maps while making classification decisions, visualizing the Raman shifts that the CNN network focuses on when making classification decisions.

Results and discussion

Fabrication and characterization of the FA@tPF substrate

The magnetic SERS substrate FA@tPF was synthesized through a stepwise assembly process designed to enhance its performance for uranyl ion detection. The synthesis began with the coating of Fe_3O_4 nanoparticles with a silica layer (SiO_2) to improve stability and surface functionality, followed by modification with positively charged PDDA, enabling the subsequent electrostatic adsorption of negatively charged Au nanoparticles (AuNPs) to form the FA substrate. Subsequently, tPF, a COPs material derived from polyarylene ether (PAE), was synthesized on the FA substrate surface, resulting in the formation of the final FA@tPF composite (Fig. 1). The introduction of the PAE structure imparts exceptional chemical and thermal stability to the substrate, ensuring robust performance under harsh environments such as acidic, alkaline, and seawater conditions, as supported by previous studies and our experimental findings[25]. We hypothesize that upon exposure to a uranyl solution, the FA@tPF substrate efficiently captures uranyl ions through the abundant active adsorption sites provided by the tPF layer, facilitating their proximity to the Au surface. This interaction significantly enhances the local concentration of uranyl ions at the SERS 'hot spots', thereby amplifying the Raman signal intensity. Consequently, the FA@tPF substrate exhibits strong potential as a stable, sensitive, and selective platform for the detection of uranyl ions, even in complex environmental matrices. In addition, the uranyl–FA@tPF interaction can be efficiently reversed using Na_2CO_3 solution, enabling potential substrate regeneration. Combined with portable Raman detection and data-driven machine learning analysis, this system offers practical advantages for on-site and intelligent monitoring of uranyl species.

To assess the suitability of the FA@tPF substrate for SERS applications, its structural and chemical properties were thoroughly characterized. The synthesis strategy integrates Fe_3O_4@SiO_2 magnetic microspheres, SERS-active Au nanoparticles, and a tPF functional layer, ensuring a robust and efficient substrate for uranyl ion detection. Supplementary Fig. S1 shows the hysteresis loops of FA and FA@tPF. Both materials exhibit superparamagnetic behavior. Meanwhile, FA@tPF retains a high saturation magnetization (Ms) value of 38.5 emu·g^{-1}, indicating that the introduction of the tPF layer does not significantly compromise the magnetic responsiveness of the material. The SEM image (Fig. 2a) reveals that the Fe_3O_4@SiO_2 particles exhibit a uniform spherical morphology, while TEM analysis (Fig. 2b, c; Supplementary Fig. S2) confirms the successful deposition of Au nanoparticles on the surface, forming the FA composite. The addition of the tPF layer is validated by TEM elemental mapping (Fig. 2d–g), which demonstrates the homogeneous distribution of Au, C, O, and N elements across the substrate, highlighting the uniform coating of tPF. This uniform distribution is critical for ensuring consistent SERS-active sites and enhancing detection sensitivity.

Further spectroscopic analyses substantiate these findings. FT-IR spectra (Fig. 2h) display characteristic peaks at 2,218 cm^{-1} (C≡N) and 1,030 cm^{-1} (C–O), confirming successful functionalization of the FA substrate with the tPF layer[23]. The high-resolution XPS of the total spectrum further supports this conclusion, with a peak of 687.76 eV attributed to F elements from tPF (Supplementary

https://doi.org/10.48130/scm-0026-0023

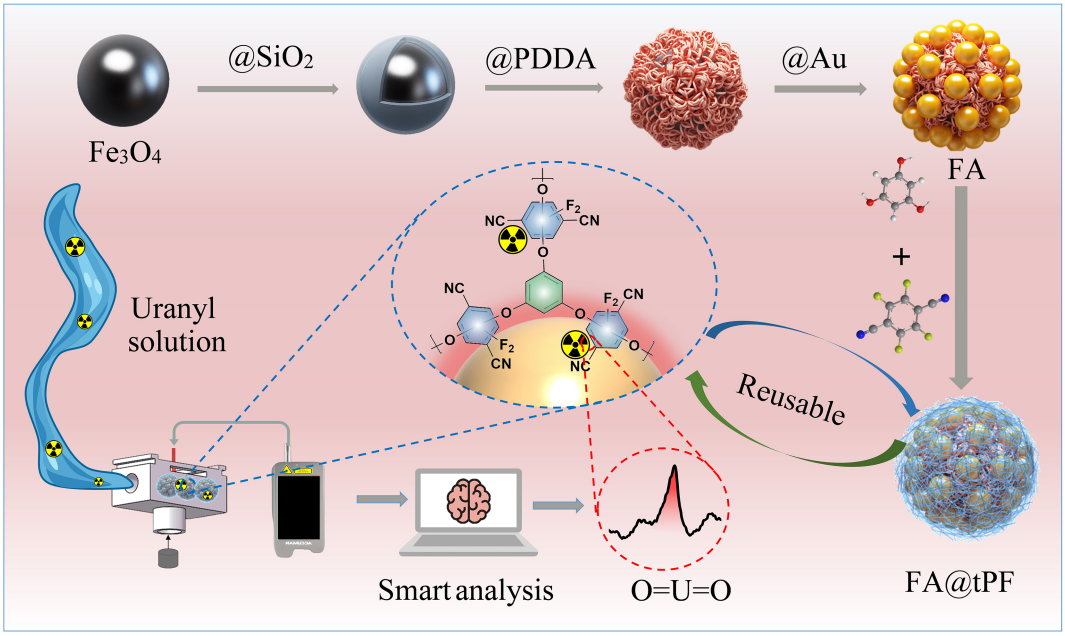

Fig. 1 Schematic representation of the synthesis and detection process of the FA@tPF nanocomposite. Fe_3O_4 nanoparticles were sequentially modified with SiO_2, PDDA, Au, and tPF ligands. The composite enables uranyl ion adsorption, Na_2CO_3-assisted regeneration, portable SERS detection, and machine-learning based spectral analysis.

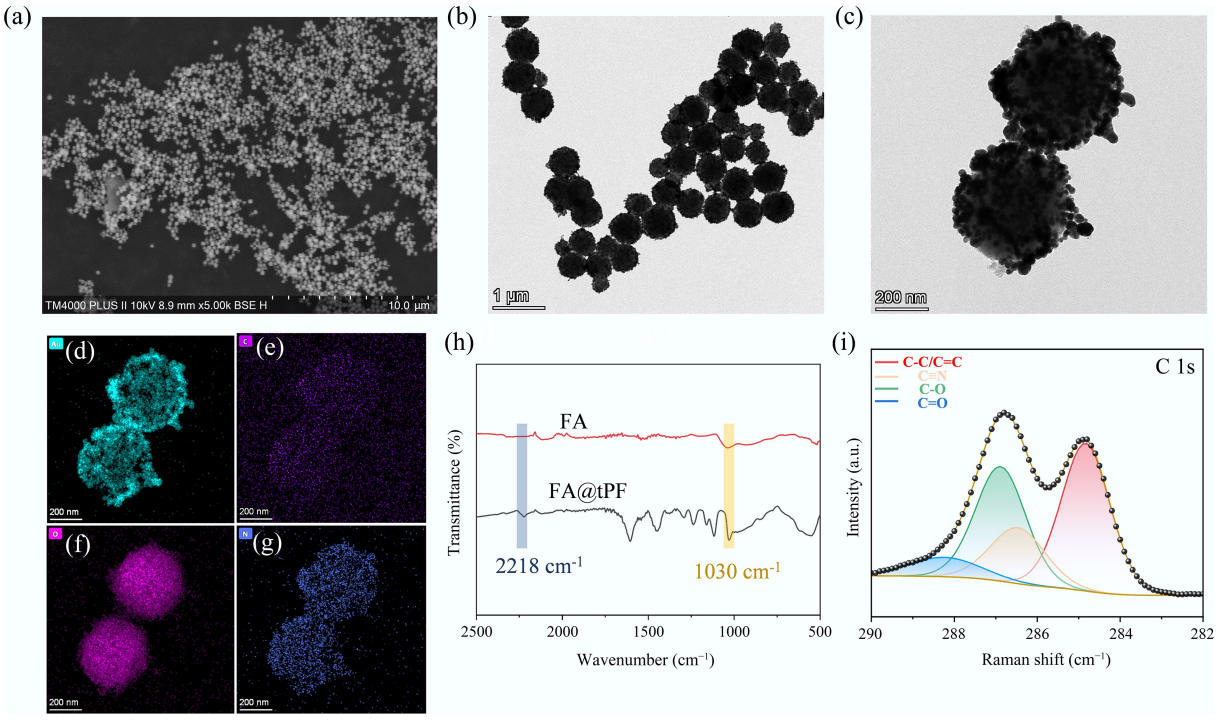

Fig. 2 (**a**) SEM image of Fe_3O_4@SiO_2; (**b**), (**c**) TEM images of FA, and FA@tPF substrates; (**d**)–(**g**) TEM image of FA@tPF with elemental mappings for Au, C, O and N; (**h**) FT-IR spectra of FA and FA@tPF; (**i**) XPS spectra of FA and FA@tPF.

Fig. S3)[26]. Additionally, the deconvolution of the C 1s spectrum (Fig. 2i) reveals peaks at 286.9 and 286.4 eV, corresponding to the C–O and C≡N bonds within the aromatic ether framework, which are signatures of the tPF structure[26–28]. These results collectively confirm the successful synthesis of the FA@tPF substrate, endowing it with tailored morphological and chemical properties that are ideal for the sensitive and selective detection of uranyl ions via SERS.

Sensitivity of the FA@tPF substrate

The sensitivity of FA@tPF was evaluated using two Raman probes, CV and 4-MPY. For CV, characteristic Raman peaks at 1,178, 1,587, and 1,616 cm^{-1} were clearly observed (Fig. 3a, b), consistent with previously reported data[29,30]. Notably, the FA@tPF substrate successfully detected the peak at 1,178 cm^{-1} at a low concentration of 10^{-8} $mol{\cdot}L^{-1}$ (Fig. 3b), while the limit of detection (LOD) for the unmodified FA was

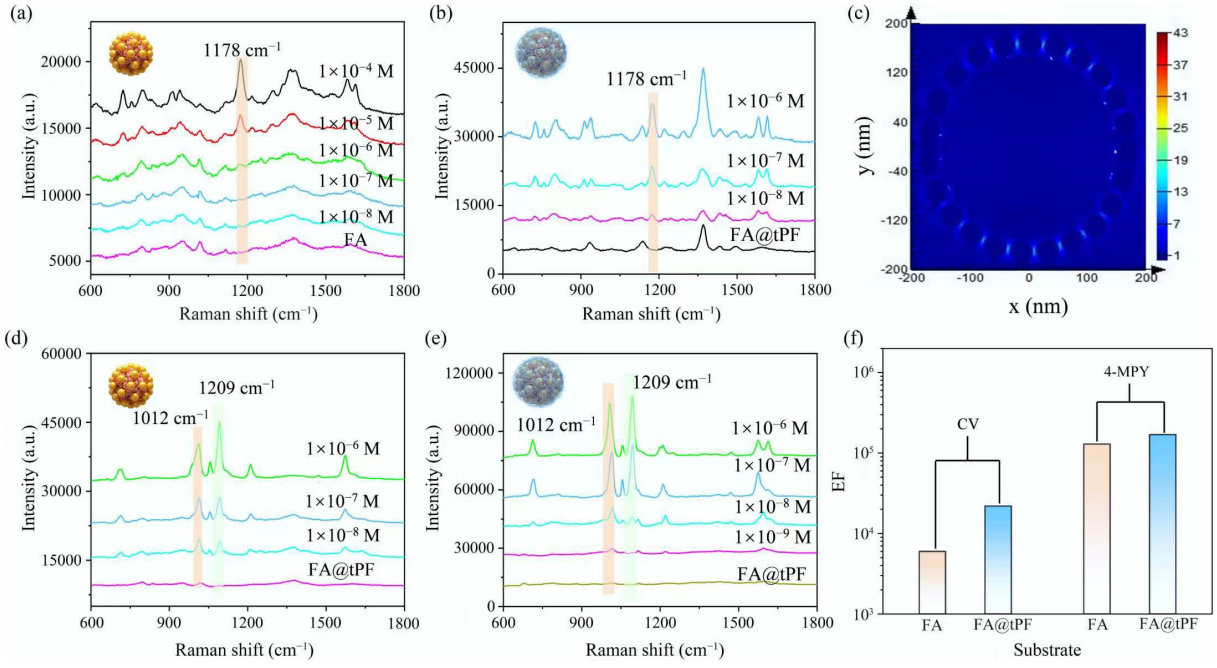

Fig. 3 (**a**), (**b**) SERS spectra of CV on FA and FA@tPF substrates at concentrations to 1×10^{-8} and 1×10^{-4} mol·L^{-1}; (**c**) electromagnetic field simulation of FA; (**d**), (**e**) SERS spectra of 4-MPY on FA and FA@tPF substrates at concentrations from 1×10^{-9} to 1×10^{-6} mol·L^{-1}; (**f**) enhancement factors (EF) of FA and FA@tPF for detecting CV and 4-MPY.

only 10^{-6} mol·L^{-1} (Fig. 3a). This significant improvement highlights the signal enhancement effect of the tPF layer. The electromagnetic field simulation (Fig. 3c) further supports this observation, revealing strong localized field enhancement around the Au nanoparticles, which is crucial for amplifying the SERS signal. The calculated enhancement factor (EF) for CV on the FA@tPF reached 2.2×10^4, which is approximately 3.7 times higher than that of the unmodified FA substrate (6×10^3) (Fig. 3f).

For 4-MPY, characteristic Raman peaks were observed at 1,012, 1,094, and 1,209 cm^{-1} (Fig. 3d, e), with an LOD of 1×10^{-8} mol·L^{-1} for both FA@tPF and FA substrates. Although the tPF layer exhibited a more pronounced effect for CV detection, it had a relatively smaller impact on 4-MPY, with the FA@tPF substrate still achieving a slightly higher EF compared to the unmodified FA (Fig. 3f). This result suggests that the tPF functionalization significantly enhances the sensitivity of the FA substrate for CV detection, while maintaining efficient performance for 4-MPY. These findings confirm the FA@tPF substrate as a versatile and robust platform for the trace detection of multiple analytes, demonstrating its broad applicability in SERS-based sensing.

Mechanism of uranyl ion detection by FA@tPF

To evaluate the effectiveness of the FA@tPF substrate for detecting uranyl ions (UO_2^{2+}), a comparative analysis of SERS spectra before and after tPF coating was conducted. Figure 4b shows a broad and asymmetric band at 850 cm^{-1} in the SERS spectrum of the FA@tPF substrate upon uranyl ion detection, which is in line with previous literature reports (Supplementary Table S1). The calculated LOD for uranyl ions was determined to be 1×10^{-7} mol·L^{-1}. Meanwhile, the limits of detection (LOD) among different batches were consistent at 1×10^{-7} mol·L^{-1} (Supplementary Fig. S4), demonstrating the excellent detection sensitivity and reproducibility of the substrate. In contrast, the unmodified FA substrate failed to detect uranyl peaks even at 1×10^{-4} mol·L^{-1} (Fig. 4a), which is attributed to the weak interaction between the FA substrate and uranyl ions, as well as the inherently small Raman scattering cross-section of uranyl, making detection challenging. Therefore, the correlation between the intensity of the characteristic peak at 850 cm^{-1} and the logarithm of concentration[31] (1×10^{-7} to 1×10^{-4} mol·L^{-1}), was evaluated (Fig. 4c). The results demonstrate a strong linear relationship ($R^2 = 0.9977$), confirming the reliability of the substrate for trace-level uranyl detection. Therefore, tPF modification of the FA surface is essential for uranyl SERS detection, which also reflects the unique interaction of uranyl with the substrate through a change in peak position. Meanwhile, a flow cell was employed to simulate the detection of actual flowing samples (schematic shown in Fig. 4d). As depicted in Fig. 4e, at a uranyl concentration of 1×10^{-5} mol·L^{-1}, the characteristic peak intensity increased gradually with extended flow time, though it remained lower than that under direct shaking conditions. Consequently, 20 min were chosen as the flow detection time; the detection limit test (Fig. 4f) yielded a value of 1×10^{-7} mol·L^{-1}, demonstrating that the simulated real-world detection performance matched that of laboratory conditions.

To further elucidate the specific role of the FA@tPF substrate in detecting UO_2^{2+}, its adsorption mechanism was systematically analyzed using various spectroscopic techniques. The schematic in Fig. 5a illustrates the adsorption and detection mechanism of the FA@tPF substrate toward uranyl, demonstrating that uranyl ions generate enhanced Raman signals through interactions with Au NPs, with a characteristic peak at 850 cm^{-1} in the SERS spectrum. FT-IR spectroscopy and XPS were further used to investigate this adsorption mechanism. FT-IR analysis (Fig. 5b) shows a new absorption band at 911 cm^{-1} following uranyl adsorption, confirming chemical bond formation between UO_2^{2+} and the substrate. XPS analysis characterized the elemental valence states before and after uranyl adsorption. As depicted in Fig. 5c, the comprehensive XPS profile is presented, with a particular emphasis on the detailed profiles of U (Fig. 5d). The zeta potential of the FA@tPF was measured to be −22.5 mV (Supplementary Fig. S5), indicating a

https://doi.org/10.48130/scm-0026-0023

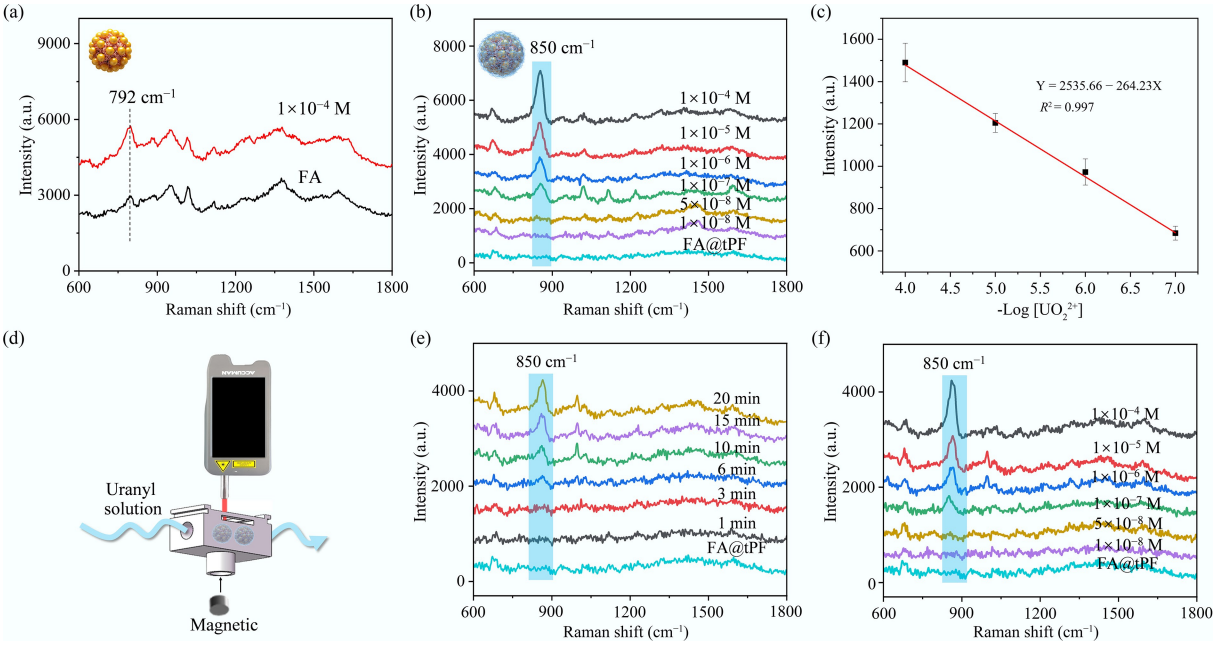

Fig. 4 (**a**) SERS spectra of 1 × 10^{-4} mol·L^{-1} UO_2^{2+} on FA substrates; (**b**) SERS spectra of uranyl ions at concentrations between 1 × 10^{-8} and 1 × 10^{-4} mol·L^{-1} on FA@tPF substrates; (**c**) linear fit for uranyl ion detection via SERS on FA@tPF; (**d**) schematic diagram of the flow cell; (**e**) Raman spectra at a concentration of 1 × 10^{-5} mol·L^{-1} as a function of flow time; (**f**) Raman spectra of the flow cell under flow conditions for 20 min at concentrations ranging from 1 × 10^{-8} to 1 × 10^{-4} mol·L^{-1}.

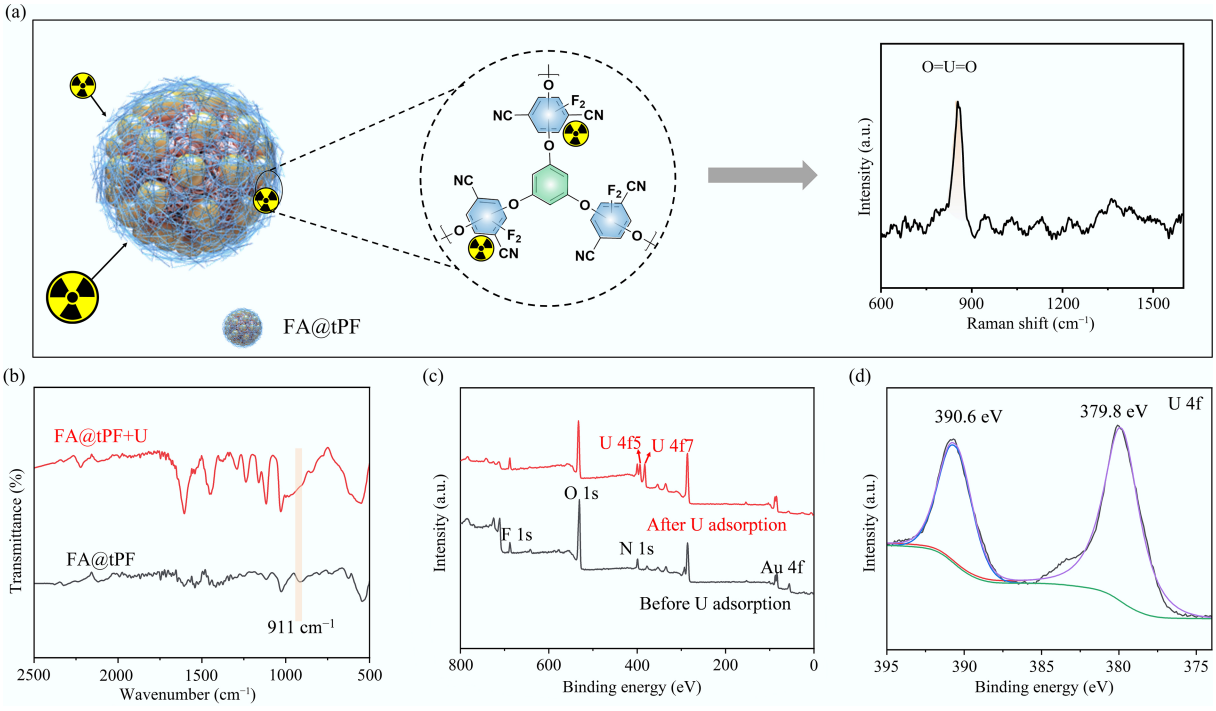

Fig. 5 (**a**) Schematic illustration of the uranyl ion detection mechanism on FA@tPF substrate. (**b**) FT-IR spectra of FA@tPF before and after U(VI) adsorption; (**c**) XPS survey spectra showing elemental changes on FA@tPF before and after uranyl adsorption; (**d**) U 4f for FA@tPF after uranyl loaded.

negatively charged surface, which may facilitate electrostatic interactions with uranyl ions. These results indicate that the FA@tPF substrate interacts strongly with uranyl ions primarily through coordination interactions, while electrostatic attraction may also contribute, enabling efficient adsorption and enhanced SERS signals.

Practical applicability and intelligent recognition performance of FA@tPF for uranyl ion detection

The practical applicability of the FA@tPF substrate for detecting UO_2^{2+} in complex aqueous environments was evaluated through interference experiments with various coexisting ions, including common metal

ions (Mg^{2+}, Na^{+}, Ca^{2+}, K^{+}, Zn^{2+}, Mn^{2+}) and anions (NO_3^{-}, SO_4^{2-}). The 850 cm^{-1} characteristic peak remained stable at 10^{-4} $mol{\cdot}L^{-1}$ UO_2^{2+} concentration (Fig. 6a), indicating minimal impact from the interfering ions and highlighting the substrate's excellent selectivity and anti-interference capability. The substrate's long-term stability was further confirmed by monitoring signal intensity under varying NaCl concentrations (Supplementary Fig. S6) and repeated spectral scans over time (Fig. 6b), where consistent SERS signals were maintained. These findings demonstrate that the FA@tPF substrate exhibits robust performance, high sensitivity, and excellent stability, making it a reliable platform for practical uranyl detection in complex environmental systems.

The reusability of the FA@tPF substrate was assessed via multiple adsorption and desorption cycles, using Na_2CO_3 as an eluent. Efficient desorption was evidenced by the disappearance of SERS peaks after elution and their reappearance upon re-adsorption (Fig. 6c; Supplementary Fig. S7). The SERS signals remained stable over the initial cycles, indicating robust recovery without significant degradation. Over six cycles, the characteristic peaks remain clearly detectable, with only a slight decrease in intensity after repeated use (Supplementary Fig. S8), demonstrating good signal stability and retention[23]. Furthermore, TEM images (Supplementary Fig. S9a) show that the overall morphology of the FA@tPF substrate remains unchanged after the elution process, indicating that the core–satellite structure is well preserved. FT-IR spectra (Supplementary Fig. S9b) further indicate that the characteristic functional groups of the tPF layer remain largely unchanged after regeneration, suggesting that the COP functional layer is not significantly affected during the desorption process. The regeneration mechanism is illustrated in Fig. 6d: uranyl ions interact strongly with the tPF-modified FA substrate, and treatment with Na_2CO_3 effectively disrupts these interactions, releasing the bound ions and restoring the substrate for reuse. This efficient regeneration process preserves both the structural integrity and detection capability of the FA@tPF substrate, making it a viable, cost-effective platform for practical applications in environmental monitoring.

To assess the spectral reliability and AI-readiness of the newly developed FA@tPF substrate, we compared it with the unmodified FA and the previously reported FA@ZIF-8[17]. PCA conducted on the uranyl SERS spectra from all three substrates (Fig. 6e) revealed that FA@tPF exhibited the most compact clustering in PCA space, indicating superior signal uniformity. To further demonstrate intelligent detection capabilities, the FA@tPF substrate was integrated with a CNN model for automated classification of spectra before and after uranyl adsorption. The CNN achieved 100% accuracy (Fig. 6f), highlighting its strong ability to capture uranyl-induced spectral changes. Furthermore, to interpret the model's decision-making process, Grad-CAM was employed to generate a spectral importance heatmap, reflecting the relative contribution of different spectral regions to the model's decision, which identified the 850 cm^{-1} uranyl peak as the dominant contributor to classification (Supplementary Fig. S10). These results confirm that the model relies on chemically meaningful features rather than random noise. The high classification accuracy of the CNN model is attributed to the clear spectral distinction before and after uranyl adsorption on the FA@tPF, demonstrating that the substrate supports intelligent AI-assisted detection with strong reliability.

Both the newly developed FA@tPF substrate in this work and our previously reported FA@ZIF-8 significantly enhanced the SERS sensitivity for uranyl detection compared to the bare FA, achieving comparable detection limits down to 1×10^{-7} $mol{\cdot}L^{-1}$, which is slightly below the US EPA's maximum contaminant level for uranium in drinking water, 30 $\mu g{\cdot}L^{-1}$ (~1.26×10^{-7} $mol{\cdot}L^{-1}$). It is worth noting that this detection limit was obtained under a 20-min flow-based enrichment condition. Given the magnetic solid-phase

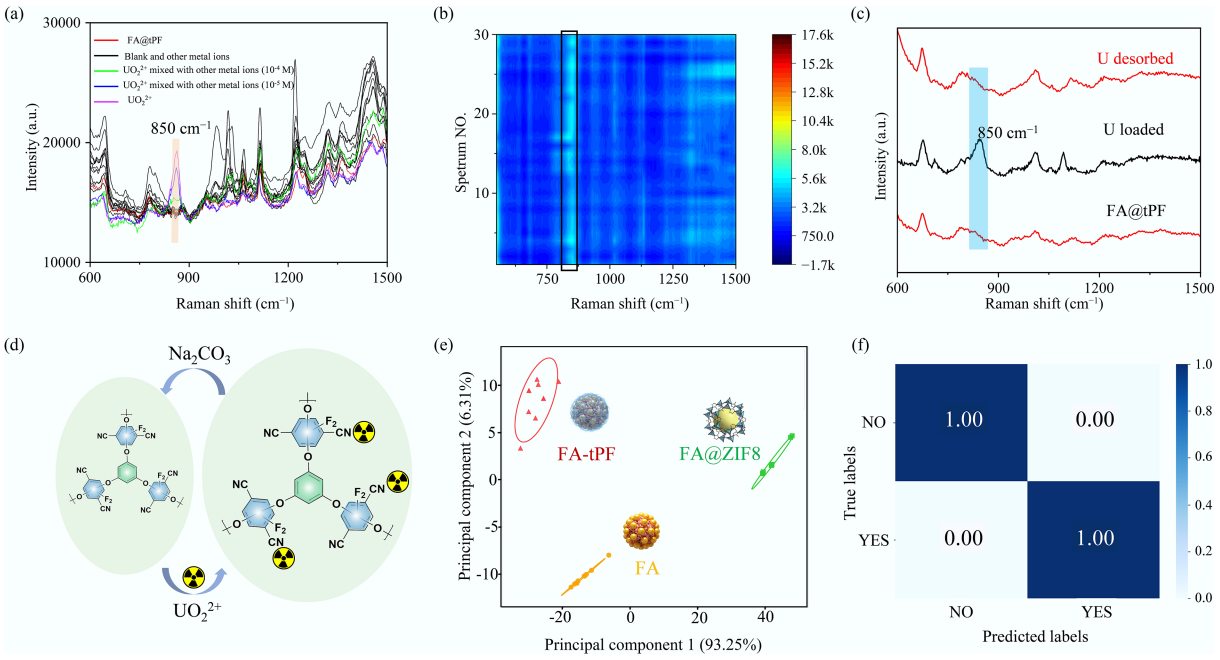

Fig. 6 (**a**) SERS spectra of FA@tPF for detecting uranyl ions in the presence of various interfering ions; (**b**) SERS spectra of FA@tPF before and after elution using Na_2CO_3; (**c**) SERS spectra of FA@tPF before and after one adsorption and desorption cycle; (**d**) schematic illustration of the regeneration mechanism of FA@tPF substrate with Na_2CO_3; (**e**) principal component analysis (PCA) plot of 10^{-5} $mol{\cdot}L^{-1}$ uranyl SERS spectra collected from FA, FA@ZIF-8, and FA@tPF substrates; (**f**) classification confusion matrix of SERS spectra before and after adsorption of uranyl on FA@tPF substrate by a CNN classification model.

microextraction functionality of the platform, prolonged enrichment could theoretically enable even lower detection thresholds. While both FA@ZIF-8 and FA@tPF showed similar sensitivity, FA@tPF exhibited a clear advantage in reusability, maintaining consistent SERS performance over multiple adsorption and desorption cycles. In particular, it could be efficiently regenerated using Na_2CO_3 without observable signal loss. This recyclability feature enhances the practical utility of FA@tPF and supports its potential as a sustainable and field-deployable SERS platform for real-world uranyl monitoring.

Conclusions

We developed a reusable magnetic SERS substrate, FA@tPF, that enables sensitive and selective UO_2^{2+} detection. The tPF modification significantly enhances SERS performance, achieving a detection limit of 1×10^{-7} mol·L^{-1} under a 20 min enrichment condition, with potential for further improvement through prolonged magnetic extraction. Comprehensive characterization demonstrated the successful synthesis of the FA@tPF substrate, highlighting its strong chemical stability, uniform morphology, and abundant active sites. The substrate exhibited excellent selectivity in the presence of coexisting ions and maintained consistent performance over multiple adsorption and desorption cycles with Na_2CO_3-assisted regeneration. Beyond high analytical performance, the platform incorporates machine learning algorithms including PCA, CNN, and Grad-CAM for spectral classification and mechanistic interpretation. These findings highlight the potential of FA@tPF for integration into intelligent sensing networks, enabling sustainable, real-time uranium surveillance, and contributing to the advancement of nuclear environmental safety.

Supplementary information

It accompanies this paper at: https://doi.org/10.48130/scm-0026-0023.

Author contributions

The authors confirm their contributions to the paper as follows: Wentao Zhang: investigation and writing – original draft; Jing Ma: investigation and data curation; Yiyan Zhang: investigation and data curation; Suhua Wang: review and editing; Muhammad Wakeel: review and editing; Zhenli Sun: conceptualization, funding acquisition and writing – original draft. All authors reviewed the results and approved the final version of the manuscript.

Data availability

The datasets used or analyzed during the current study are available from the corresponding author on reasonable request.

Funding

This work was supported by the National Natural Science Foundation of China (Grant No. U21A20290).

Declarations

Competing interests

The authors declare that they have no known competing financial interests or personal relationships that could have appeared to influence the work reported in this paper.

Author details

[1]MOE Key Laboratory of Resources and Environmental System Optimization, College of Environmental Science and Engineering, North China Electric Power University, Beijing 102206, China; [2]School of Environmental Science and Engineering, Guangdong University of Petrochemical Technology, Maoming 525000, China; [3]Department of Environmental Sciences COMSATS University Islamabad, Vehari Campus, Vehari 61100, Pakistan

References

[1] Sholl DS, Lively RP. 2016. Seven chemical separations to change the world. *Nature* 532(7600):435–437
[2] Chen T, Yu K, Dong C, Yuan X, Gong X, et al. 2022. Advanced photocatalysts for uranium extraction: Elaborate design and future perspectives. *Coordination Chemistry Reviews* 467:214615
[3] Yadav S, Choudhary N, Sonpal V, Vyas BG, Paital AR. 2025. Sunlight-mediated photocatalytic uranium extraction from seawater: a bio-resistant heterojunction for highly selective uranium sensing and extraction with *in vivo* application. *Journal of Materials Chemistry A* 13(5):3858–3871
[4] Ma M, Wang R, Xu L, Xu M, Liu S. 2020. Emerging health risks and underlying toxicological mechanisms of uranium contamination: lessons from the past two decades. *Environment International* 145:106107
[5] Sun Z, Liao Y, Zhang Y, Sun S, Kan Q, et al. 2025. Sustainable carbon materials in environmental and energy applications. *Sustainable Carbon Materials* 1:e007
[6] Tai X, Sun Z. 2025. Extra-high extraction of uranium from seawater by covalent organic frameworks through structure geometry and functional active site modification. *Sustainable Carbon Materials* 1:e006
[7] Zhang L, Levy I, Vassileva E. 2023. Determination of uranium isotopes in marine sediments and seawaters by SF ICP-MS after rapid chemical separation using TK200 resin. *Environmental Science and Pollution Research* 30(15):44671–44683
[8] Bettinelli M, Spezia S, Minoia C. 2004. Analysis of uranium and isotopic ratio measurement in fish and marine invertebrates from the North Adriatic Sea by inductively coupled plasma mass spectrometry. *Rapid Communications in Mass Spectrometry* 18(4):465–468
[9] Santos JS, Teixeira LSG, dos Santos WNL, Lemos VA, Godoy JM, et al. 2010. Uranium determination using atomic spectrometric techniques: an overview. *Analytica Chimica Acta* 674(2):143–156
[10] Sanyal K, Khooha A, Das G, Tiwari MK, Misra NL. 2017. Direct determination of oxidation states of uranium in mixed-valent uranium oxides using total reflection X-ray fluorescence X-ray absorption near-edge spectroscopy. *Analytical Chemistry* 89(1):871–876
[11] Wang S, Jiang J, He X, Yang S, Wu H, et al. 2022. Research progress of SERS on uranyl ions and uranyl compounds: a review. *Journal of Materials Chemistry C* 10(11):4006–4018
[12] Kim NH, Hwang W, Baek K, Rohman MR, Kim J, et al. 2018. Smart SERS hot spots: single molecules can be positioned in a plasmonic nanojunction using host–guest chemistry. *Journal of the American Chemical Society* 140(13):4705–4711
[13] Zhang X, Young MA, Lyandres O, Van Duyne RP. 2005. Rapid detection of an *Anthrax* biomarker by surface-enhanced Raman spectroscopy. *Journal of the American Chemical Society* 127(12):4484–4489
[14] Sun Z, Wang N, Zhang Y, Ji X, Hong Z, et al. 2024. SERS hotspot engineering using external field assembly of a plasmonic magnetic nanocomposite with high sensitivity and uniformity. *Journal of Materials Chemistry A* 12(28):17151–17157
[15] Sun C, Dong W, Peng J, Wan X, Sun Z, et al. 2020. Dual-mode fluorescence–SERS sensor for sensitive and selective detection of uranyl ions based on satellite Fe_3O_4-Au@CdTe nanostructure. *Sensors and Actuators B: Chemical* 325:128644
[16] Wen X, Liu Y, Zhang W, You L, Cai N, et al. 2025. Recyclable NiO/g-C_3N_4/ag hybrid substrates for sensitive SERS detection and photodegradation of residual pesticides in beverages. *Food Chemistry* 464:141935

[17] Wang N, Du J, Li X, Ji X, Wu Y, et al. 2023. Magnetic MOF substrates for the rapid and sensitive surface-enhanced Raman scattering detection of uranyl. *Analytical Chemistry* 95(34):12956−12963

[18] Wang Y, Li H, Tan Z, Yu J, Zhao X, et al. 2025. MOF-in-cavity structure with co-location effect of hotspots and molecules suitable for both *ex-situ* and *in-situ* SERS detections. *Sensors and Actuators B: Chemical* 440:137883

[19] Langer J, Jimenez de Aberasturi D, Aizpurua J, Alvarez-Puebla RA, Auguié B, et al. 2020. Present and future of surface-enhanced Raman scattering. *ACS Nano* 14(1):28−117

[20] Chen A, Gui Y, Luo K, Cai N, Li J. 2026. A highly sensitive SERS sensor based on magnetic-enrichment Ag@Fe_3O_4/UiO-66-NH2 for detection and solar photo-reduction of hexavalent chromium in water environment. *Talanta* 297:128702

[21] Skorjanc T, Shetty D, Valant M. 2021. Covalent organic polymers and frameworks for fluorescence-based sensors. *ACS Sensors* 6(4):1461−1481

[22] Xiao SJ, Qiu AT, Li HH, Wang MP, Zhang L, et al. 2023. Simultaneous detection and separation of uranium based on a fluorescent amidoxime-functionalized covalent organic polymer. *Spectrochimica Acta Part A: Molecular and Biomolecular Spectroscopy* 289:122182

[23] Leng R, Sun Y, Wang C, Qu Z, Feng R, et al. 2023. Design and fabrication of hypercrosslinked covalent organic adsorbents for selective uranium extraction. *Environmental Science & Technology* 57(26):9615−9626

[24] Sun Z, Du J, Duan F, He K, Jing C. 2018. Simulation and synthesis of Fe_3O_4–Au satellite nanostructures for optimised surface-enhanced Raman scattering. *Journal of Materials Chemistry C* 6(9):2252−2257

[25] Guan X, Li H, Ma Y, Xue M, Fang Q, et al. 2019. Chemically stable polyarylether-based covalent organic frameworks. *Nature Chemistry* 11(6):587−594

[26] Moulder JF, Stickle WF, Sobol WM, Bomben KD. 1992. *Handbook of X-ray photoelectron spectroscopy*. Eden Prairie, Minnesota: Perkin-Elmer Corporation, Physical Electronics Division. 261 pp

[27] D'Anna E, De Giorgi ML, Luches A, Martino M, Perrone A, et al. 1999. Study of C–N binding states in carbon nitride films deposited by reactive XeCl laser ablation. *Thin Solid Films* 347(1−2):72−77

[28] Ech-chamikh E, Essafti A, Ijdiyaou Y, Azizan M. 2006. XPS study of amorphous carbon nitride (a-C:N) thin films deposited by reactive RF sputtering. *Solar Energy Materials and Solar Cells* 90(10):1420−1423

[29] Chen LY, Yu JS, Fujita T, Chen MW. 2009. Nanoporous copper with tunable nanoporosity for SERS applications. *Advanced Functional Materials* 19(8):1221−1226

[30] Tian H, Zhang N, Tong L, Zhang J. 2017. *In situ* quantitative graphene-based surface-enhanced Raman spectroscopy. *Small Methods* 1(6):1700126

[31] He X, Zhou X, Liu Y, Wang X. 2020. Ultrasensitive, recyclable and portable microfluidic surface-enhanced Raman scattering (SERS) biosensor for uranyl ions detection. *Sensors and Actuators B: Chemical* 311:127676